Materials and Design 51 (2013) 25–33

Contents lists available at SciVerse ScienceDirect

Materials and Design

journal homepage: www.elsevier.com/locate/matdes

AA7075 bit for repairing AA2219 keyhole by filling friction stir welding

Bing Han [a], Yongxian Huang [a,*], Shixiong Lv [a], Long Wan [a], Jicai Feng [a], Guansheng Fu [b]

[a] State Key Laboratory of Advanced Welding and Joining, Harbin Institute of Technology, Harbin 150001, People's Republic of China
[b] Csr Zhuzhou Electric Locomotive Co., Ltd., Zhuzhou 412001, People's Republic of China

ARTICLE INFO

Article history:
Received 16 January 2013
Accepted 27 March 2013
Available online 6 April 2013

Keywords:
Filling friction stir welding
Aluminum bit
Keyhole
Interface
Mechanical property

ABSTRACT

In the present study, 7.8 mm thick AA2219 rolled plates were successfully filling friction stir welded (FFSW) without keyhole using a semi-consumable tool. The influences of the bit's geometric parameters and the plunge speed on the joint's mechanical properties were investigated. Microstructure of the joint, especially at the interface, was observed. The results revealed that the AA7075 bit's employment was able to decrease the shedding bit material effectively. During tensile tests, the maximum ultimate tensile strength (UTS) and elongation of the joint were 179.6 MPa and 13.7%, equivalent to 96.6% and 99% of the original defect-free friction stir welding (FSW) joint, respectively. The defect-free FFSW joints were produced at lower plunge speeds, and the fracture locations were at the softened region within the heat affected zone (HAZ) adjacent to the thermo-mechanically affected zone (TMAZ) on the retreating side. With increasing the plunge speed, the fracture location was more mainly dependent on the interface strength instead of the hardness distribution.

1. Introduction

Nowadays, high strength aluminum alloys have been applied as high strength-to-weight ratio materials [1]. Among them, the high-strength precipitate hardening Al–Zn–Mg–(Cu) 7000-series aluminum alloys such as AA7075 are extensively used in automotive and aerospace structures for their lightweight and high strength [2]. And the heat treatable Al–Cu 2000-series aluminum alloys such as AA2219 also has a great potential for a wide range of applications owing to their high specific-strength, good fracture toughness and excellent stress-corrosion resistance too [3,4].

Friction stir welding (FSW), a solid-state process invented at TWI (Cambridge, United Kingdom), in 1991, is being targeted by the industry for structurally demanding applications to provide high-performance benefits [5,6]. This new technology can join difficult to weld aluminum alloys by traditional fusion techniques, for example alloys belonging to the 2000-series with limited weldability and the 7000-series generally not recommended for welding and joining, even if they are the more used aluminum alloys in aerospace applications [7]. FSW is shown not to cause severe distortion and residual stresses generated are low compared to the traditional welding processes [6]. Weld defects, however, like groove, cavity and kissing bond are easily formed under improper parameters or technological conditions [8–10]. Emphatically, the keyhole inevitably remains at the end of the weld, from which the non-consumable welding tool entry probe has to be withdrawn after FSW or friction stir spot welding (FSSW). Both lap shear and cross-tension strengths are limited due to the relatively small bonding widths [11]. In view of the keyhole or other defects, the re-FSW process is feasible to restore the defects not only outside but also inside of the joints. However, new keyholes would be emerged as soon as the defects were repaired [12].

Up to now, a variety of methods and apparatuses have been developed to repair the keyhole in FSW welds. A solid state joining process called friction taper plug welding (FTPW) or friction hydro pillar processing (FHPP) has been invented by TWI during the 1990s, which involves drilling a tapered through hole into a plate. After that, a tapered plug with a similar included angle is friction welded to the matching surface of the hole in a few seconds by forcing the rotating plug against the drilled hole [13,14]. It can be used in several applications, for example, at the location of a defect or crack in offshore steel and aerospace aluminum structures that is intended to be repaired [15,16]. However, due to the use of the tapered plug without shoulder, stress concentration is going to be formed at the interface, and a tapered through hole and proper plug should be prepared to get defect free joints, especially for high melting point material thick structures due to the high flow stress.

Furthermore, a novel apparatus called auto-adjusting pin tool has been developed by the National Aeronautics and Space Administration, which can be used for materials of varying thickness, and the pin can be incrementally withdrawn from the work pieces during the final stage of the transverse, thus eliminating the exit keyhole in the weld [17]. And similarly, the retractable [18,19] or double acting re-filling tool [20], consisting of a separated outer

* Corresponding author. Tel.: +86 451 86413951; fax: +86 451 86416186.
E-mail address: yxhuang@hit.edu.cn (Y. Huang).

0261-3069/$ - see front matter Crown Copyright © 2013 Published by Elsevier Ltd. All rights reserved.
http://dx.doi.org/10.1016/j.matdes.2013.03.089

shoulder and an inner pin, has been developed and applied to eliminate the keyhole by controlling the relative movement of shoulder and pin at the final stage of welding. Uneconomically, all these three similar welding tools must be installed on exceedingly complex and expensive equipments.

In addition to the above, a new solid state spot joining process called friction bit joining (FBJ) has been developed relying on a special designed consumable joining bit [11,21,22]. The bonding widths of the joints have been increased. The lap shear strength of the FBJ spot is better than that of the self-piercing rivets, and the FBJ is especially applied to join soft and hard materials combinations, such as AA5754 and DP980 steel [22]. The FBJ process is carried out in two main steps: a cutting step and a joining step. During the cutting phase, the bit cut through the top layer of the two sheets to be joined. The heat is mainly generated by the friction between the bit and surrounding sheet materials. The bit is consumed as filler material that joins the sheets together. At the end of the joining phase, the spindle of the welding machine is stopped very rapidly and then restarted to separate the joining bit from the weld [11,21,22].

Recently, a new technique called self-refilling friction stir welding (SRFSW) has been proposed by Zhou et al. [23], where conventional FSW process is transformed by adopting a series of non-consumable polycrystalline cubic boron nitride (PCBN) tools with gradual change in geometry. Keyholes in 316L stainless steel plates left by friction stir processing (FSP) process have been successfully refilled by combined plastic deformation and flow of the material around the keyhole using the designed tools step by step. Tensile test results show that the tensile specimens are fractured at the BM side, and the relative tensile strength and

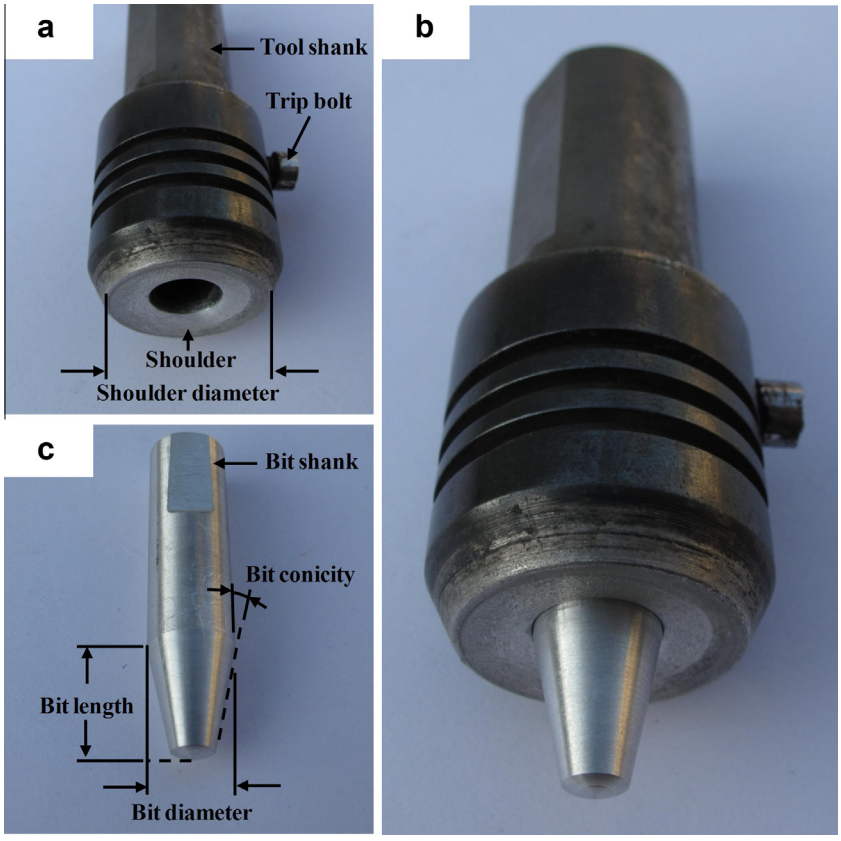

Fig. 1. Features of FFSW tool: (a) steel shoulder, (b) AA7075 bit and (c) assembled semi-consumable FFSW tool.

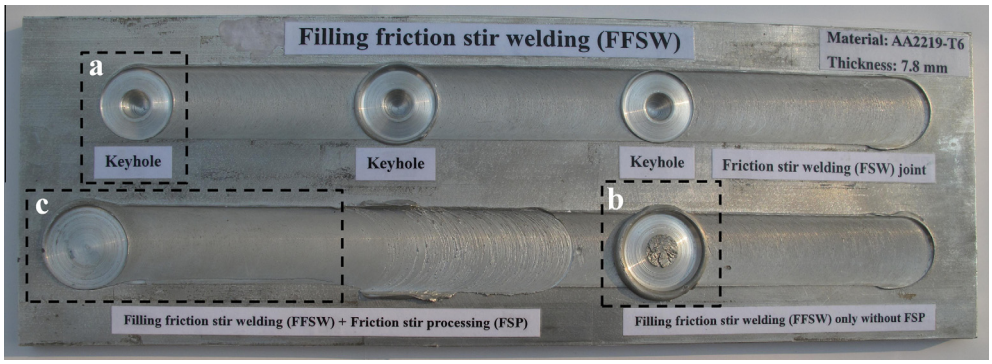

Fig. 2. Dissimilar AA2219/AA7075 FFSW plates with (a) FSW keyhole defects, (b) repaired keyhole and (c) repaired keyhole after FSP.

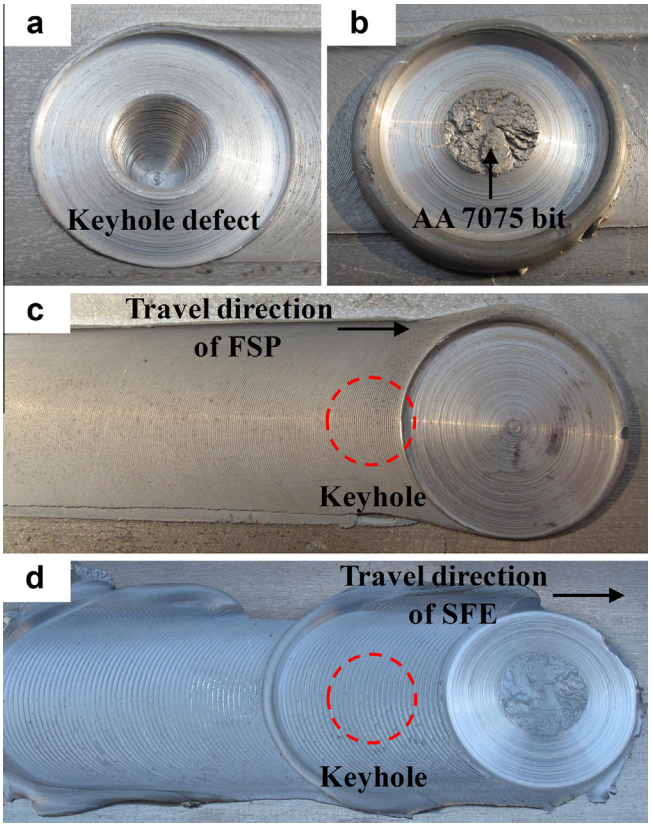

Fig. 3. Detailed images of FFSW plates: (a) keyhole defects, (b) repaired keyhole, (c) repaired keyhole after FSP and (d) repaired keyhole after SFE.

elongation of the refilled joint are 112% and 82% of that of the BM respectively [23].

In our previous articles [24–26], a new technique of filling friction stir welding (FFSW) had been presented. Based on FSW conventional cylindrical welding tool, a new specially FFSW welding tool using a consumable tapered AA2219 joining bit, instead of the original non-consumable stir probe with relatively smaller diameter, fixed in a concentric larger diameter steel shoulder. The features of this FFSW tool are illustrated in Fig. 1 and its key geometric descriptions are shown in this picture. By this new method, typical FSW keyhole in the weld can be successfully removed based on the principle of solid-state joining without defect. A friction stir welded plate containing filling friction stir welds is shown in Fig. 2. Detailed views of the keyhole defect and the weld after FFSW repair are shown in Fig. 3, items a and b, respectively. And by tests, the FFSW joint's average values of ultimate tensile strength (UTS) and elongation are 172 MPa equal to 90% of FSW weld strength and 11.2% equal to 82% of FSW weld elongation, respectively. Furthermore, under the optimized parameters of welding process and joining bit's geometric features, the highest UTS can reach 174.7 MPa, nearly 95% of FSW weld's value, and the highest elongation is about 14.2%, close to FSW weld's value. Quasi equivalence mechanical performances without weld defects have been achieved by FFSW joint with excellent interface and mechanical properties [24–26]. However, during previous FFSW process, as the bit keeping inserting downward into the keyhole, the bit head begins to contact the zigzag structures on the keyhole's surface. Consequently, material deformation and fierce attrition will be happened at the contact region. Additionally, resulting from the relative lower hardness (96 $HV_{250\ g}$) and the keyhole's friction, part of bit's superficial material will be stripped off and fell down into the bottom of the keyhole. This experimental phenomenon can be proved in previous microstructure images located at the bottom of the filled zone (FZ) [25]. In micro-images, a noticeable structure characterized by several overlapped materials has been observed because of the bit shedding materials. However, the problem is that these overlapped materials can be the potential defect sources of cavity and flaw. As a result of the features of the FFSW tool, the material at the bottom of the FZ experiences relatively gentle stir and insufficient heating especially compared with the weld nugget zone (WNZ), and the defects like cavity and flaw are easy to be formed locating at interlayer or interface between two adjacent layers. So, the bottom of the FZ must be a potential weak region and further experiments of FFSW using new harder joining bits are meaningful and rich prospects. Above problems can be hopefully improved and even solved ideally due to this innovative idea.

In the present work, a harder AA7075-T6 bit was applied to repair the AA2219-T6 keyhole of FSW beam. Six kinds of AA7075-T6 bits were designed and applied in this paper. Four different plunge speeds were selected, ranging from 0.5 to 8 mm min^{-1}, to prove if FFSW efficiency can be further improved and increased without joint properties' degradation. The investigation of the dissimilar alloys FFSW joint was initiated with three objectives. To investigate the practicability of the AA2219/AA7075 FFSW joint and the characteristics of joint's macro/microstructure. Basing on the previous experiments, to design series of AA7075 bits with selected geometric sizes and examine the mechanical properties of the joint mainly in terms of tensile strength, elongation and hardness distributions under different plunge speeds. Finally, to analyze and summarize the effects of the bit's geometric features and plunge speed on joint's mechanical properties.

2. Experimental procedures

Following the previous work, in this paper, the base material (BM) tested for this investigation was still the commercially produced AA2219 with the following chemical composition: Cu 6.8, Si 0.49, Mn 0.32, Fe 0.23, Zr 0.2, V 0.08, Ti 0.06, Zn 0.04 and balance Al (all in mass%). The alloy was hot-rolled in plate of 7.8 mm thick and subjected to a normal T6 temper treatment (solutionised at 535 °C for 4 h, water quenched and aged at 185 °C for 24 h) [24,25]. Interestingly, AA7075-T6 barstock with an original diameter of 12 mm was selected as the new bit raw material. The chemical compositions and mechanical properties of AA7075 and AA2219 are listed in Table 1. Obviously, with a higher hardness 110 HV_{250g}, AA7075 bar is harder than AA2219 rolled plate (94 HV_{250g}). The gage dimension of the weld specimen was 300 mm in length and 100 mm in width respectively and sliced using electrical discharge machining. Before FSW, the upper surfaces and edges of the strips were polished by wire brush and cleaned by acetone solution to avoid parent material surface oxide film and oil stain. Then the samples were clamped to the backing plate under the facility. Both FSW and FFSW processes were performed using a FSW facility (FSW-3LM-003, China FSW Center, Beijing FSW Technology Ltd., Beijing, China). In FSW, a conventional alloy steel tool and a series of optimal weld parameters used in previous work were selected [25]. The welding tool was rotated in the clockwise direction. The joining conditions including FSW tool's sizes and weld parameters are listed in Table 2. In FFSW, an innovative semi-consumable tool consisting of a consumable AA7075 bit and a high-speed steel (HSS) shoulder were used to remove keyhole and defects. The repairing conditions including FFSW tool's geometric dimensions and weld parameters are reported in Table 3. Emphatically, like previous experiments, six kinds of AA7075 bits with same selected geometric parameters were used in present work. Additionally, four increasing gradually plunge speeds (0.5,

Table 1
Chemical composition (wt.%) and mechanical properties of AA7075 bit and AA2219 base metal.

Materials	Chemical compositions (wt.%)										UTS (MPa)	Elongation (%)	Hardness (HV)
	Si	Fe	Cu	Mn	Mg	Cr	Zn	Ti	Zr	Al			
AA7075	0.08	0.17	1.50	0.04	2.81	0.19	5.82	0.02	0.01	Bal.	–	–	110
AA2219	0.49	0.23	6.8	0.32	0.02	–	0.04	0.06	0.2	Bal.	280	14.1	94

Table 2
Friction stir welding conditions.

Tool size	Shoulder diameter, mm	22
	Probe diameter, mm	9.8
	Probe length, mm	7.6
	Probe conicity, degree	15
Material of tool		HSS
Rotary speed, rpm		800
Welding speed, mm min^{-1}		500
Plunge speed, mm min^{-1}		3.0
Deep indentation depth, mm		0.2
Tilt angle, degree		2.5 (forward)

Table 3
Filling friction stir welding conditions.

Tool size	Shoulder diameter, mm	22
	Bit diameter, mm	10
	Bit length, mm	10, 11, 12
	Bit conicity, degree	11, 12
Material of tool		HSS, AA7075
Rotary speed, rpm		800
Welding speed, mm min^{-1}		500
Plunge speed, mm min^{-1}		0.5, 2, 5, 8
Deep indentation depth, mm		0.1
Tilt angle, degree		2.5 (forward)

2, 5, 8 mm min^{-1}) were adopted and as a result, the highest efficiency of FFSW can be increased to 40 s. The whole process of FFSW can be mainly decomposed into three parts, namely previous FFSW, shoulder further effect (SFE) and lastly friction stir processing (FSP) [25]. In SFE and FSP, the weld parameters include rotary speed (800 RPM), traverse speed (500 mm min^{-1}), deep indentation depth (0.1 mm) and tilt angle (2.5°). In SFE, the plunge speed keeps fixed 0.5 mm min^{-1} without any change. Features of the typical weld in SFE and FSP are shown in Fig. 3, items d and c, respectively. The exact positions of the keyholes are marked by red dashed lines. Dissimilar materials of AA2219 BM and AA7075 bit were successfully joined by FFSW and no superficial porosity or defects were observed on weld surface.

The specimens for both macro and microstructural characterization were cross- sectioned perpendicular to the weld line. Macrostructure images were performed by a stereoscopic microscope (SM, Olympus-SZX12) and microscopy observations were performed by an optical microscope (OM, Olympus-MPG3). Before analysis, the metallographic specimens were prepared by sand papers grinding, diamond paste (1 μm) polishing and Keller's reagent (1 ml hydrofluoric acid, 1.5 ml hydrochloric acid, 2.5 ml nitric acid and 95 ml water) etching. Visual inspection of joints was also carried out in order to distinguish defects on the weld surface.

Tensile tests were performed at an initial strain rate of 10^{-3} s^{-1}, using a universal testing machine (Instron-5569), in order to evaluate the mechanical properties of the joints obtained by FFSW of AA7075 bit and AA2219 BM under different welding conditions including bit's shape and plunge speed. The tensile specimens were sectioned in the transverse direction respect to the weld line using an electrical discharge machining (EDM). The transverse tensile specimens with a gauge length of 40 mm, a width of 15 mm and a thickness of 7.8 mm were prepared with reference to China National Standard GB/T 2650-2008 (equivalent to ISO 9016: 2001) [27]. All the specimens were mechanically polished before tests in order to eliminate the effect of possible surface irregularities and stress concentration. The tensile tests were carried out at room temperature, and at least 96 h after FFSW when the alloy reached a naturally aged stable condition [25]. After tensile tests, the fracture surfaces were examined using a scanning electron microscope (SEM, Hitachi-570).

In microhardness tests, Vickers microhardness distribution maps were measured on the cross section perpendicular to the welding direction using a computerized digital microhardness tester (HVS-1000) under a load of 250 g for 10 s. As schematically shown in Fig. 4, a total of four test lines were measured across the cross-section at an interval of 2 mm, and the interval between two adjacent indentations on one line is 1 mm, with a total of 160 indentations.

3. Results and discussion

3.1. Macro and microstructures of FFSW joints

Fig. 5 shows the typical cross-sectional macrograph of the AA2219/AA7075 FFSW joint welded under a plunge speed of 0.5 mm min^{-1} and using an AA7075 bit (10 mm in length and 11° in conicity). It can be seen that no welding defect (groove, cavity and kissing bond) is detected on this joint. Like previous work, with suitable bits and plunge speeds, the filling materials are sufficient and excellent bonding interface can be achieved. Compared with the traditional FSW joints' structure, the generalized profile of the FFSW joint can be normally divided into several similar typical zones, i.e. the WNZ at the weld center, the HAZ surrounding the WNZ, the TMAZ between the WNZ and the HAZ, and the BM. The FZ, however, which is totally different from the traditional zones, is observed in the center of the FSSW joint under the WNZ. Obviously, the FZ is formed by the AA 7075 bit. Furthermore, the self-refilling friction stir welding (SRFSW) joints' structure can be generally divided into three regions, the typical refilled zone

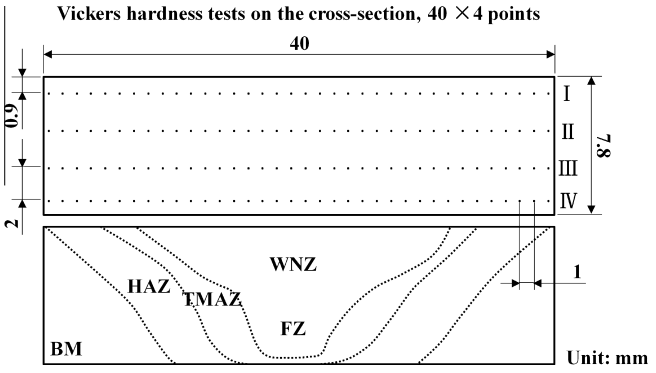

Fig. 4. Schematic illustration of the FFSW joint for microhardness tests, together with an indication of various zones across the weld (BM, HAZ, TMAZ, WNZ and FZ).

(RZ), the TMAZ and the BM, without the WNZ. Similarly, the RZ is mainly formed by PCBN tool's pin as the refilling material [23]. And in friction taper plug welding (FTPW), three macro-regions can be easily identified in its solid state joints: the BM, the TMAZ and plug material [15]. However, due to the use of the tapered plug without shoulder's effect, the WNZ cannot be observed, either.

Fig. 6 shows the interface in details between the FZ and the highly deformed and stirred TMAZ by OM, in four positions: the advancing side (6a), the retreating side (6b and d) and the keyhole's bottom (6c). Obviously, as a result of shoulder and AA7075 bit's abundant stir and materials' deformation, the interface in WNZ is not discernible, AA7075 bit and AA2219 BM have been metallurgical bonded very well. The transition between the FZ and the TMAZ is very well defined, containing classical formation of the elliptical "Onion-ring" structure parallel to the interface. Compared with the interface closer to the keyhole's bottom shown in Fig. 6d, the interface on both sides adjacent to the WNZ (Fig. 6a and b) is more diffused. As arrowed in Fig. 6c, shedding bit material is still existent at the bottom of the keyhole. In FFSW, as the tool plunging downward and the AA7075 bit entering into the keyhole, the head of the bit begins to contact with the inner surface of the keyhole, the bit surface material will be gradually scraped down into the keyhole's bottom under fierce grinding between bit's head and keyhole's inner face. This shedding material, on a certain extent, will change the shape of bit's head and affect the bottom interface's formation negatively.

To observe more clearly, Fig. 7 presents higher magnification interface images of two selected regions A and B labeled in Fig. 6c and d respectively. Like FSW, for the FFSW joint bonded by thick plates, the shoulder frictional heat source cannot equably transfers to the middle part and the bottom region at thickness direction. In the lower part of thick joints, the heat input is in direct proportion to the material deformation extent and frictional heat. Therefore, the less homogeneously temperature distributes along

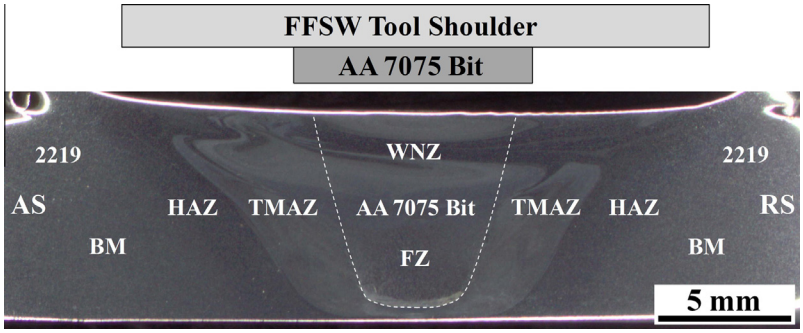

Fig. 5. Cross-section of the representative defect-free FFSW joint using AA7075 bit.

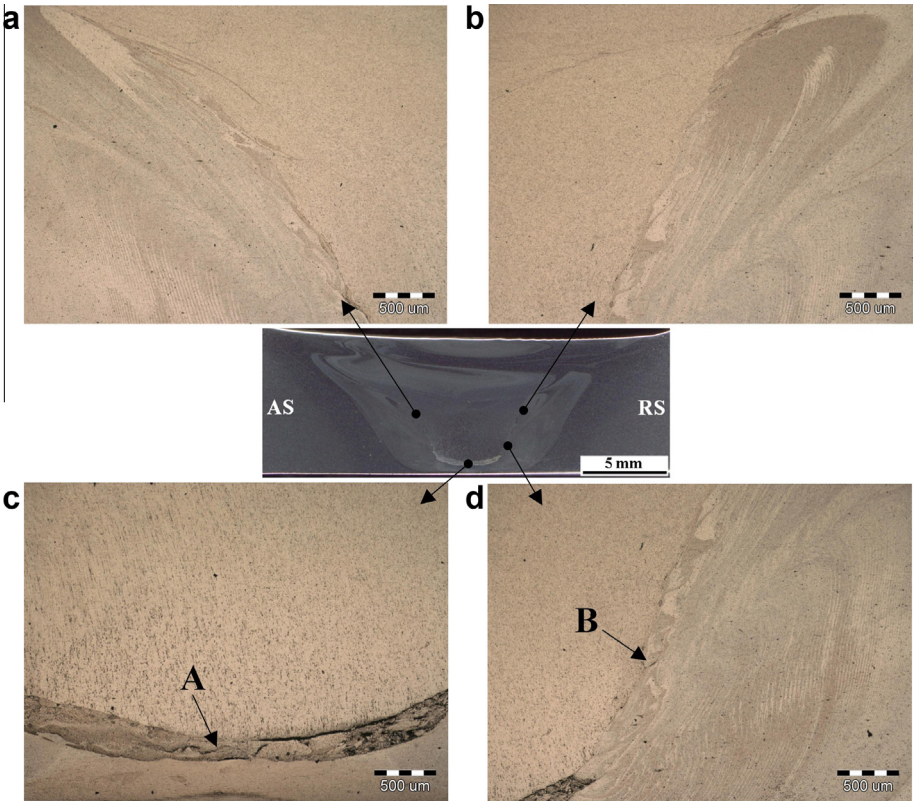

Fig. 6. Optical micrographs of the representative FFSW joint's interface between TMAZ and WNZ (FZ), indicating: (a) on the advancing side, (b and d) on the retreating side, and (c) on the bottom of the keyhole.

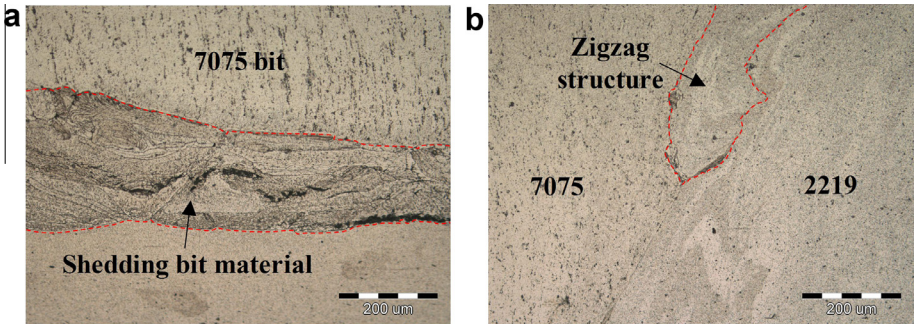

Fig. 7. High magnification images of the FFSW joint's interface at selected areas: (a) region A in Fig. 6c and (b) region B in Fig. 6d.

the joint thickness direction, the less material plastic deformation occurs around the bit during FFSW for thick plates. If the workpiece material at the bit/keyhole interface was lack of heat input and plastic deformation, porosity defect like void could be easily formed. As arrowhead and dashed line shown in Fig. 7a, the shedding bit material is evident between the keyhole's bottom and the AA7075 bit's head. Several layers of scraped materials accumulate together periodically, and meanwhile, welding defects like void (dark slender regions in Fig. 7a) and flaw can be formed within different stack layers. As shown in Fig. 7b, without sufficient friction stir heat input energy of the shoulder and the AA7075 bit, the interface close to the keyhole's bottom is distinguishable. Deformation and plastic flow of bit and material around the keyhole are limited and inadequate comparing with those within the WNZ. Notably, the zigzag structure, which is formed during former FSW process, can still be found in this region.

3.2. Tensile properties

Fig. 8 shows the transverse tensile results of the AA2219/AA7075 FFSW joints plotted against the plunge speed. Six kinds of selected AA7075 bits with regular geometric parameters are used in FFSW process. Except the plunge speed, all these FFSW

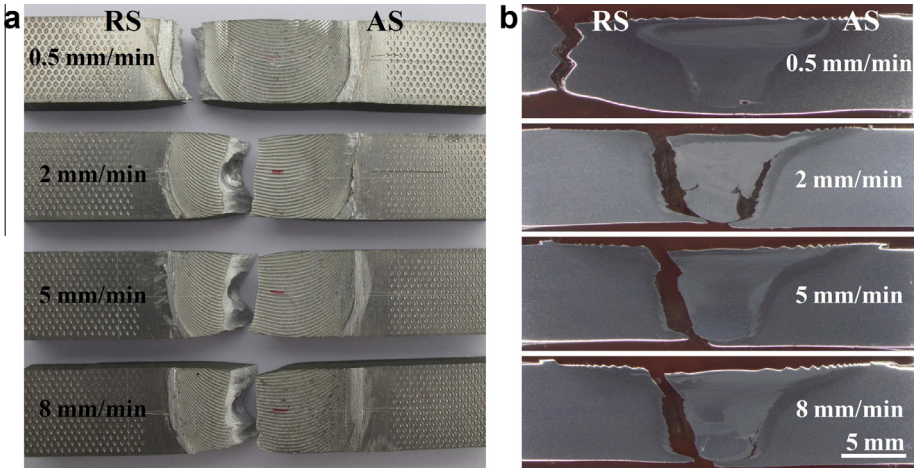

Fig. 8. Mechanical properties of the joints welded by different AA7075 bits and under different plunge speeds: (a) tensile strength and (b) percentage of elongation.

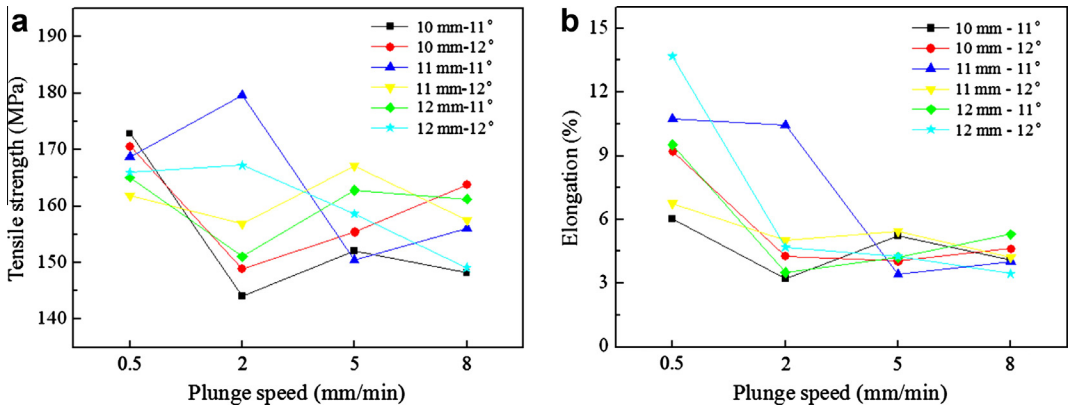

Fig. 9. Fracture features of the joints welded at different plunge speeds: (a) tensile specimens and (b) cross-sections.

joints are welded under the same optimized parameters listed in Table 3. Experimental results show that the plunge speed has a notable significant effect on joint's strength and ductility. Obviously, all joints have lower UTS and elongation than BM's listed in Table 1. As shown in Fig. 8a, the joint's UTS declines unsteadily with increasing the plunge speed gradually. The maximum UTS is 179.6 MPa, equivalent to 96.6% of the original no defect weld, using the bit of 10 mm in length and 11° in conicity, under a plunge speed of 2 mm min^{-1}. In contrast to the variation trend in strength, as shown in Fig. 8b, the joint's elongation declines sharply with increasing the plunge speed from 0.5 to 2 mm min^{-1} due to the presence of void defects. However, large fluctuation cannot be observed in spite of the plunge speed's continued increase from 2 to 8 mm min^{-1}. The maximum elongation is 13.7%, close to the original weld's value, using the bit of 12 mm in length and 12° in conicity, under a plunge speed of 2 mm min^{-1}. For the original FSW weld, the average values of UTS and elongation are 65.6% and 97.2% of the BM respectively. The synergetic restrictions of UTS and elongation allow the plunge speed not to increase higher than 2 mm min^{-1}. To make comparisons with SRFSW [23] on joints' tensile properties, the optimal relative elongation of the FFSW joints (over 90% of the BM's) is a little higher than that of the SRFSW joints (only 82% of the BM's). However, as a result of the differences of these two techniques mainly on keyholes' geometrical sizes and original welds' strengths, the maximum relative UTS of the FFSW joints is lower than that of the SRFSW joints. It is important to note that, the keyholes refilled during SRFSW process are all formed by former FSP, and the keyholes' geometrical sizes like diameter and depth are obviously much less than those of the keyholes formed by former FSW before FFSW. It is easy to realize that the relative strength of the weld containing the keyhole is going to be reduced with the increase of the keyhole's geometrical sizes. So, the geometrical sizes of the original keyholes are significant influencing factors that causing the differences between FFSW and SRFSW on the joints' relative UTS.

Fig. 9 reveals the tensile fracture features of the FFSW joints welded at various plunge speeds, using the bits of 10 mm in length and 12° in conicity. From the front face graph (see Fig. 9a), significant necking exists around the fracture locations, which means that the macroplastic deformation occurs in the joints during tensile tests. The fracture locations are apparently parameter dependent and all joints are fractured on the retreating side (RS). The specific fracture position can be observed in Fig. 9b. The joint welded at the lowest plunge speed of 0.5 mm min^{-1} tends to be fractured in the HAZ, and a void can be observed at the bottom of the interface (see Fig. 9a). As the plunge speed further increases from 2 to 8 mm min^{-1}, however, the void defect is formed between the bit and the keyhole, resulting in the fracture locations shifted from the HAZ to the interface on the same side. Comparing Fig. 9 with Fig. 8b, it is obvious that if the joint was fractured at interface area, then its elongation would be badly deteriorated.

3.3. Fractography

The fracture surfaces of tensile tested specimens are characterized using SEM to understand the failure patterns. On a macroscopic scale, Fig. 10a shows a cross-sectional SEM macrograph of the fractured AA2219/AA7075 FFSW joint welded at a plunge speed of 5 mm min^{-1} and using the bit of 11 mm in length and 11° in conicity. Fig. 10b presents a comparison of the fractograph features of the original AA2219 FFSW joint with the same plunge speed and bit. Obviously, these two joints' fracture surfaces are both characterized by fine dimples and tearing ridges, which are created generally in ductile fracture and indicating extensive plastic deformation. As a consequence of employing higher plunge speed, these two joints are both fractured on the interface of the bit and the keyhole, and the bits' profile can be observed clearly. As arrowed in Fig. 10b, a big piece of the shedding AA2219 bit material is exposed on the bottom of the keyhole. Expectedly, in a certain extent, the employment of new AA7075 bit results in an effective decrease of the shedding bit material (arrowheads in Fig. 10a). Different from AA2219 joint's fracture surface shown in Fig. 10b, it can be seen that the exposed AA7075 bit surface is mainly divided into two different zones, as marked with A and B in Fig. 10a and their magnified SEM graphs are shown in Fig. 10c and d respectively. One zone magnified in Fig. 10c is characterized

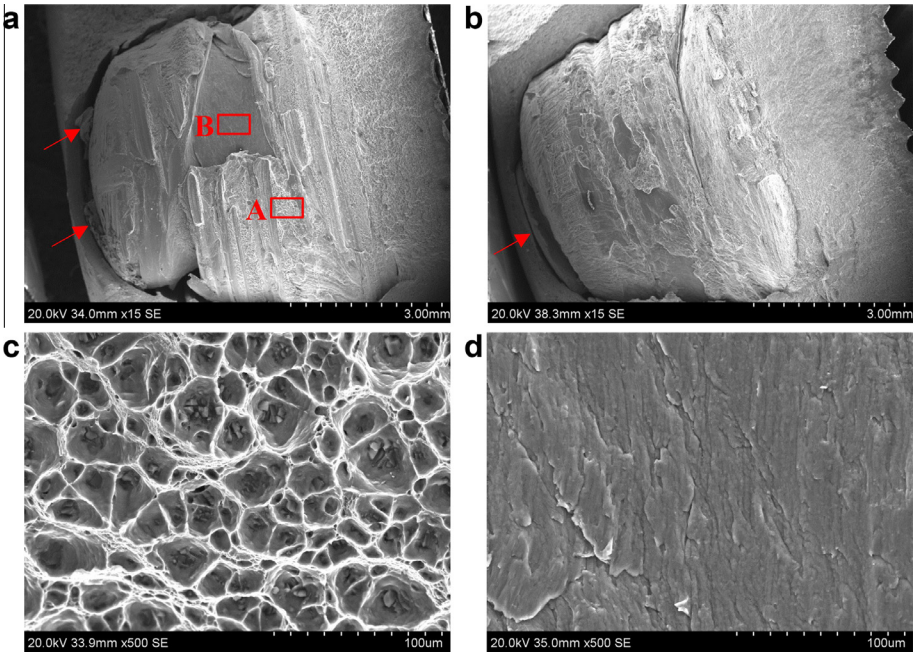

Fig. 10. SEM images showing fracture surfaces features of the samples taken from the FFSW joints in tensile tests, indicating: (a) overall morphology of the AA2219/AA7075 FFSW joint, (b) overall morphology of previous AA2219 FFSW joint, (c) micrograph of A zone, and (d) micrograph of B zone.

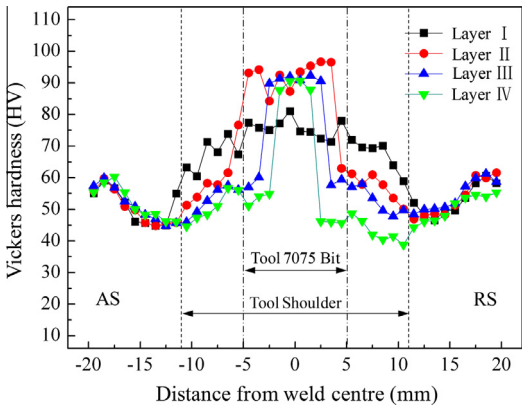

Fig. 11. Vickers hardness profiles across the weld region for a typical FFSW joint at four different layers.

by a number of deep equiaxed dimples of varying sizes and shapes, and cracked second-phase particles, this zone should be the sufficient melting, extruding and stirring zone. However, because of AA7075 relative aggravated ductility, another zone magnified in Fig. 10d is characterized by much smoother and flatter surface which is caused by the crush of the bit surface material. These observations suggest that the metallurgical bonding is really existed within almost the whole region of the AA2219/AA7075 FFSW joint.

3.4. Microhardness profile

Fig. 11 shows the typical microhardness profiles across the AA2219/AA7075 FFSW joint shown in Fig. 5 on four different lines through the thickness of the plate, one near the shoulder, two at mid-thickness and a fourth measurement near the weld root, as schematically shown in Fig. 4. The average hardness of the whole weld region on four lines is lower than the BM's (94 $HV_{250\ g}$). In a certain extent, the hardness curves are symmetrical with respect to the weld centerline. The hardness first decreases from the BM to a lowest value and then shows an increase towards the weld center. Consequently, all hardness profiles present a 'W' type. The lowest hardness (38.8 $HV_{250\ g}$) lies in the HAZ adjacent to the TMAZ on the RS. As mentioned before, the tensile properties and fracture locations of the joints are dependent on the hardness distributions and the weld defects positions [28]. The joint welded under lower plunge speed 0.5 mm min^{-1} is fractured within the softened region in the HAZ on the RS. However, as the plunge speed increasing, the defects are much easier to be formed at the interface and resulting in the shift of the fracture location from the softened region to the interface on the same side (Fig. 8). Additionally, the hardness near the centerline of the weld, especially in the FZ, still closes to the original values of the AA7075 raw material without significant change.

4. Conclusions

In summary, a mixed AA2219/AA7075 FFSW joint was successfully welded employing a semi-consumable tool consisting of an alloy steel shoulder and an AA7075 bit. The effects of varying bit geometric parameters and plunge speeds on the joint's strength, ductility, fracture features and hardness distributions were determined. The joints' UTS, especially elongation, decreased with increasing plunge speed. The joints' maximum UTS and elongation were 179.6 MPa and 13.7%, equivalent to 96.6% and 99% of the original defect-free weld's values respectively. Compared with original AA2219 bit, the AA7075 bit's employment could effectively decrease the bit's shedding material in the keyhole. The fracture surface was characterized by fine dimples and tearing ridges. The fracture features of the joints were largely dependent on the hardness distribution and interface strength. At low plunge speed of 0.5 mm min^{-1}, the joint was fractured at the softened region within the HAZ adjacent to the TMAZ on the RS. However, at higher plunge speeds, the fracture tended to initiate at the interface on the same side because of low interface strength. Hardness maximum values were mainly concentrated around the joint center.

Acknowledgements

The work was jointly supported by the National Natural Science Foundation of China (Nos. 50904020 and 50974046) and the Fundamental Research Funds for the Central Universities (No. HIT. NSRIF. 2012007).

References

[1] Aonuma M, Nakata K. Dissimilar metal Joining of 2024 and 7075 aluminium alloys to titanium alloys by friction stir welding. Mater Trans 2011;52:948–52.
[2] Di SS, Yang XQ, Fang DP, Luan GH. The influence of zigzag-curve defect on the fatigue properties of friction stir welds in 7075-T6 Al alloy. Mater Chem Phys 2007;104:244–8.
[3] Nunes AC, Bayless EO, Jones CS, Munafo PM, Biddle AP, Wilson WA. Variable polarity plasma arc welding on the space shuttle external tank. Weld J 1984;63:27–35.
[4] Albertini G, Bruno G, Dunn BD, Fiori F, Reimers W, Wright JS. Comparative neutron and X-ray residual stress measurements on Al-2219 welded plate. Mater Sci Eng A 1997;224:157–65.
[5] Mahoney MW, Rhodes CG, Flintoff JG, Spurling RA, Bingel WH. Properties of Friction-Stir-Welded 7075 T651 Aluminum. Met Mater Trans 1998;29A:1955–64.
[6] Cavaliere P, Cerri E, Squillace A. Mechanical response of 2024–7075 aluminium alloys joined by Friction Stir Welding. J Mater Sci 2005;40:3669–76.
[7] Guerra M, Schmidt C, Mcclure LC, Murr LE, Nunes AC. Flow patterns during friction stir welding. Mater Charact 2003;49:95–101.
[8] Liu HJ, Chen YC, Feng JC. Effect of zigzag line on the mechanical properties of friction stir welded joints of an Al–Cu alloy. Scripta Mater 2006;55:231–4.
[9] Zhang H, Lin SB, Wu L, Feng JC, Ma SL. Defects formation procedure and mathematic model for defect free friction stir welding of magnesium alloy. Mater Des 2006;27:805–9.
[10] Kim YG, Fujii H, Tsumura T, Komazaki T, Nakata K. Three defect types in friction stir welding of aluminum die casting alloy. Mater Sci Eng A 2006;415:250–4.
[11] Huang T, Sato YS, Kokawa H, Miles MP, Kohkonen K, Siemssen B, et al. Microstructural evolution of DP980 steel during friction bit joining. Mater Sci Eng A 2009;40A:2994–3000.
[12] Liu HJ, Zhang HJ. Repair welding process of friction stir welding groove defect. Trans Nonferrous Met Soc China 2009;19:563–7.
[13] Dunkerton SB, Nicholas DE, Sketchley PD. Repairing defective metal workpiece – by friction welding with a metal plug. Great Britain Patent Application No. 9125978, 1991.
[14] Thomas WM, Temple-Smith P. Friction plug extrusion for solid-phase welding thick plates – by relatively moving consumable member and bore in substrate while urging them together to generate frictional heat to plasticise member. Great Britain Patent Application No. 2306365; 1997.
[15] Unfried JS, Paes MTP, Hermenegildo TFC, Bastian FL, Ramirez AJ. Study of microstructural evolution of friction taper plug welded joints of C–Mn steels. Sci Technol Weld Join 2010;15:506–13.
[16] Hartley PJ. Friction plug weld repair for the space shuttle external tank. Weld Met Fab 2002;9:6–8.
[17] Ding RJ, Oelgoetzp A. The hydraulic controlled autoadjustable pin tool for friction stir welding. US Patent No. 5893507; 1996.
[18] Su P, Gerlich A, North TH, Bendzsak GJ. Material flow during friction stir spot welding. Sci Technol Weld Join 2006;11:61–71.
[19] Allen CD, Arbegast WJ. Evaluation of friction spot welds in aluminium alloys. SAE technical paper no. 2005–01-1252, SAE International, Warrendale, PA, USA; 2005.
[20] Uematsu Y, Tokaji K, Tozaki Y, Kutita T, Murata S. Effect of re-filling probe hole on tensile failure and fatigue behaviour of friction stir spot welded joints in Al–Mg–Si alloy. Int J Fatigue 2008;30:1956–66.
[21] Miles MP, Feng Z, Kohkonen K, Weickum B, Steel R, Lev L. Spot joining of AA5754 and high strength steel sheets by consumable bit. Sci Technol Weld Join 2010;15:325–30.
[22] Miles MP, Kohkonen K, Packer S, Steel R, Siemssen B, Sato YS. Solid state spot joining of sheet materials using consumable bit. Sci Technol Weld Join 2009;14:72–7.

[23] Zhou L, Liu D, Nakata K, Tsumura T, Fujii H, Ikeuchi K, et al. New technique of self-refilling friction stir welding to repair keyhole. Sci Technol Weld Join 2012;17:649–55.
[24] Huang YX, Han B, Tian Y, Liu HJ, Lv SX, Feng JC, et al. New technique of filling friction stir welding. Sci Technol Weld Join 2011;16:497–501.
[25] Huang YX, Han B, Lv SX, Feng JC, Liu HJ, Leng JS, et al. Interface behaviours and mechanical properties of filling friction stir weld joining AA2219. Sci Technol Weld Join 2012;17:225–30.
[26] Huang YX, Han B, Lv SX, Feng JC, Leng JS, Chen XB. The technique of filling friction stir welding for repairing the keyhole based on the principle of solid state joining. Trans China Weld Inst 2012;33:5–8.
[27] GB/T 2650–2008/ISO 9016: 2001. Tensile test method on welded joints. Standardization Administration of the People's Republic of China; 2008.
[28] Liu HJ, Fujii H, Maeda M, Nogi K. Tensile properties and fracture locations of friction-stir-welded joints of 2017-T351 aluminum alloy. J Mater Process Technol 2003;142:692–6.